OPEN ACCESS
Jurnal Ilmiah Ilmu Terapan Universitas Jambi
Vol. 9 No. 3. September 2025, pp. 924-940 DOI. 10.22437/jiituj.v9i3.42846
Research Article

STUDY OF 3D PRINTING HIPS BREAST PHANTOM MATERIAL: EFFECT OF EXPOSURE VOLTAGE VARIATION AND NODULE SIZE

Mohtar Yunianto[1,*], Nanda Astika Devi[1], Fuad Anwar[1], Adnan Cindyana[2]

[1] Physics Department, Faculty of Mathematics and Natural Sciences, Sebelas Maret University, Jawa Tengah, Indonesia
[2] Postgraduate Program in Physics, Faculty of Science and Mathematics, Diponegoro University, Jawa Tengah, Indonesia
Corresponding author email: mohtaryunianto@staff.uns.ac.id

Article Info
Received: Apr 07, 2025
Revised: May 25, 2025
Accepted: Jun 18, 2025
OnlineVersion: Jul 02, 2025

Abstract
A study has examined the characteristics of 3D printer materials of HIPS and PLA. The study began by printing HIPS materials that resembled breast organs and PLA materials that resembled breast cancer nodules. Then it exposed them using a CT scan with voltage variations of 80 kV, 100 kV, and 120 kV. The parameters studied were compared with the reference breast organ. The results obtained at these voltages obtained CT-number values sequentially (-85.14±0.25) ; (-64.79±0.21) HU; (-55.08±0.18) HU values from the reference 35 to -94 HU, relative electron density values sequentially 0.915; 0.935; 0.945 with a reference value of 0.950, the density value of the material obtained is (0.921±0.002) g/, The EDG value is 3.24 x from ICRU 1989 was 3.33 x, The EDV value is (3.00 ± 0.01) x from ICRU report 44 was 3.18 x 10, the value is 3.50 the value of ICRU data is 3.28, and the effective dose values are respectively 2.53 mSv, 2.83 mSv, 3.20 mSv. Based on these characteristics, the results indicate that the breast phantom matches the characteristics of the breast organ, allowing it to be used to predict the presence of breast cancer, as it shares the same characteristics. The results of exposure to the lung cancer nodule phantom on the CT-Scan image of the 2 mm *nodule* size are not visible. The results of this study can be used as a consideration for radiologists when choosing a voltage based on the predicted size of the breast cancer nodule.

Keywords 3D Printer, Breast Phantom, CT-Number, CT-Scan, HIPS, PLA

INTRODUCTION

Cancer is one of the diseases with the highest mortality rate both in Indonesia and in the world. Cancer is a non-communicable disease characterised by abnormal growth in human body tissue cells. Cancer cells can develop and spread to other parts of the body and, in the worst conditions, can cause death (Widyanengsih et al., 2023). Cancer can be caused by unhealthy lifestyles, infections,

environmental conditions, genetic factors, and carcinogenic substances (Plummer et al., 2016; Spytska, 2025). The order of types of cancer with the highest number of new cases in Indonesia includes breast cancer, cervical cancer, and lung cancer (Utami & Saptiari, 2020; Hermanto et al., 2023). One of the cancers that is a priority in the world and Indonesia today is breast cancer (Rifda et al., 2023). According to the Global Burden of Cancer (GLOBOCAN) data, in 2022, there were 66,271 new cases of breast cancer (16.2%) of the total new cases of cancer in Indonesia, which was 408,661 cases (Globocan, 2022).

One of the causes of late treatment of cancer patients is early detection. Most cancer patients do not show early symptoms. Therefore, early detection of cancer is an effective way to diagnose it. Radiodiagnostics has an important role in the early detection of cancer (Gusriani et al., 2023). Radiodiagnostics is a diagnostic service that uses ionising radiation (X-rays). Radiodiagnostics is an examination that produces images of the human body for diagnosis/diagnosis. Radiodiagnostic X-ray machines include Computed Tomography Scan (CT-Scan), conventional radiography, and mammography (Surahmi et al., 2023).

In radiology, both diagnostic radiology and radiotherapy, radiation safety standards must be considered to obtain benefits with minimal harm for practitioners and patients. Therefore, the concept of As Low As Reasonably Achievable (ALARA) is needed, which provides the minimum dose without reducing the quality of the resulting image (Khoirot et al., 2023). Image quality is a measure of the effectiveness of the diagnosis; this is because the quality of the image results can affect the accuracy of the diagnosis (Anwar et al., 2023). Factors that affect the quality and quantity of X-ray irradiation in producing radiographic image results are called exposure factors. There are three exposure factor parameters, namely current (mA), tube voltage (kV), and exposure time (s) (Pratiwi et al., 2023; Pohan et al, 2022).

Computed Tomography Scan (CT-Scan) is an important tool in radiodiagnostics. A CT scan can diagnose tumours, cancer, sinusitis, and other conditions. CT- Scan is a radiography tool that uses high X-ray exposure to produce images of organs or the internal body (Listiyani et al., 2021). The value of the attenuation coefficient or attenuation of X-ray energy is called the CT number; the average of the X-rays determines its value. The amount of attenuation is proportional to the size of the CT number read by the detector. The unit of CT number is the Hounsfield Unit (HU), which is usually always present on X-ray machines. The HU value is the unit of X-ray attenuation after passing through an object that describes the difference in organs. In addition, the CT number also depends on the size of the marker that marks the number of pixels to be assessed (ROI). The CT range ranges from (-) 1000 HU to (+) 1000 HU. The CT number value for each tissue or organ in the human body is different, namely air -1000 HU, liver 40-60 HU, kidney 30 HU, and bones 1000 HU (Cuong et al, 2018).

A phantom is used as an organ's simulation model to research image quality and the magnitude of attenuation. A phantom is a replica of an organ or human body shape that represents various levels of tissue complexity in the human body. Phantoms can be used to provide realistic information about the human body. Phantoms are made to resemble the properties and characteristics of a tissue (Gómez & Mourão, 2022; Endra & Villaflor, 2024; Habibi et al., 2024). Radiodiagnostic phantoms validate and verify surgical, diagnostic, and radiation oncology procedure guidelines (Hatamikia et al, 2022). 3D printing is a type of additive manufacturing in which the material is arranged in layers with the help of a computer to obtain a three-dimensional (3D) shape. This technology has often been used to make phantoms. One of the advantages of using a 3D printer is that it is relatively quick to make and inexpensive compared to conventional methods. The main material for 3D printing is a filament used as a form filler. The type of filament that is often used for 3D printing includes polycarbonate, high impact polystyrene (HIPS), polylactic acid (PLA), nylon, polyethene terephthalate glycol (PETG), acrylonitrile butadiene styrene (ABS) (Riza et al., 2020).

A pulse-height spectroscopic technique accurately measured the linear attenuation coefficients of breast tissue-simulating phantom materials from 18 to 100 keV (Byng et al.,1998). A 450 ml, 45% dense breast phantom was fabricated and imaged, showing radiographic uniformity and clinically realistic appearance, though minor air bubble artefacts were noted in the EBR material (Carton et al., 2011). An interchangeable breast phantom with separate T1/T2 and diffusion units successfully mimicked tissue relaxation and ADC values across MRI systems, enabling evaluation of imaging performance and coil variability (Keenan et al.,2016). Identifying ABS, Hybrid, and PET-G as suitable substitutes for adipose, glandular, and skin tissues for use in anatomically accurate 3D-printed breast phantoms (Esposito et al., 2019). A patient-specific 3D-printed breast model was filled with silicone

and peanut oils, closely matching the T1 relaxation times of fibroglandular and adipose tissues on 3T MRI, enabling realistic MR imaging simulations (Sindi et al., 2020; Halimah et al, 2024; Jarnawi et al., 2025). Evaluated 3D-printed breast phantoms and lesions using different materials and printing methods, finding tomosynthesis images more realistic than 2D mammography, with future work focused on improving tumour print quality and quantitative assessment (Dukov et al., 2021). Epoxy–Carbopol composites with varying polymer concentrations showed attenuation and CT properties similar to human breast tissue and Perspex, making them suitable candidates for breast phantom materials (Marashdeh et al., 2023). Kunert et al. (2023) developed a breast phantom made of ABS and PMMA. ABS material was used as a substitute for adipose tissue, and PMMA was used to make glandular tissue. The breast phantom was printed with an infill density of 100%. The CT number obtained was -30 $\pm$ 10 HU. However, the ABS material experienced shrinkage during the cooling process after printing (Yang et al., 2014). In 2023, Adnan studied 3D materials printing made of HIPS. HIPS with 100% infill density and material thickness variation (2; 2.5; 3) cm have consecutive CT number values (- -62.17; -54.06; -48.72) HU. The CT number value is based on the CT number range of the breast organ, which is -35 HU to -94 HU (Yang et al., 2014).

He et al. (2019) use polyvinyl chloride (PVC) based materials and a 3D printing technique to construct a breast phantom. Eight materials suitable for 3D printing were investigated for the optimal representation of breast tissues, based on their attenuation and refractive characteristics (Malliori et al, 2020). Physical breast phantoms were printed in three components: PVA, ABS and Nylon filament materials (Franco et al., 2019). Three breast phantom models were printed in multiple resins, VeroClear, TangoPlus and Tissue Matrix (Ali et al., 2020). A breast phantom has been developed to evaluate the dose to glandular tissue during mammography directly. The results showed PLA as the most suitable 3D printing material with a dose difference of about 2.4% (Lee et al., 2020). A highly accurate 3D-printed breast surgical guide was developed and validated using a realistic MRI-based phantom, enabling precise tumour localisation for breast-conserving surgery with a mean targeting error of 2.513 ± 0.914 mm (Ock et al., 2021). Characterised over 100 tissue-mimicking breast phantom samples, demonstrating their ability to replicate various breast tissues' dielectric and mechanical properties across a wide frequency range for potential use in advanced breast cancer detection techniques (Di Meo et al., 2022).

3D printed breast phantom from polypropylene compared with the anatomical structures and associated attenuation characteristics (Schopphoven et al., 2019). Lee et al. (2021) fabricated breast phantoms by emulating glandular and adipose tissues using a 3D printer. ABS, PLAwhite, PLAorange, PET and NYLON used as adipose, glandular or skin tissue substitutes for manufacturing physical breast phantoms to measure the monoenergetic x-ray linear attenuation coefficient (Mettivier et al., 2022). A 3D printed breast phantom mounted on a commercial thoracic phantom has been developed for end-to-end testing of a novel radiotherapy technique. The phantom was validated by dose measurement and γ-analysis, showing high agreement with dose deviation <2.6% and $\gamma AS \geq 87.3\%$ (Delombaerde et al, 2020). Bellara et al (2024) determine the effective x-ray attenuation coefficient (μeff) of 3D-printing materials (PLA, ABS and HIPS). Using accessible materials and FDM 3D printing, to develop anatomical breast phantoms—basic, differential, and elastographic—for medical education and skills training in palpation, diagnosis, and tissue stiffness assessment (Leonov et al., 2023). An anthropomorphic silicone breast phantom for ultrasound-based biopsy training has been developed; The phantom exhibits good visual and tactile simulation with low production cost.(Grigorova et al., 2024). This study developed gelatin-based breast phantom materials with varying hardness and concentrations, identifying 20–25% gelatin samples as effective tissue mimics for young breast tissue in medical imaging and quality assurance (Almalky et al., 2024). developing a 3D-printed anthropomorphic breast phantom optimised for spectral photon-counting CT, using tailored imaging protocols and tissue-mimicking materials to enhance multi-energy imaging and improve diagnostic accuracy (Katsikari et al., 2024).

In 2024, Yunianto et al. conducted a test of 3D printing phantom materials, HIPS, Carbon, PLA, Nylon, and Water Washable Resin and obtained the results. The results show that HIPS, Carbon, PLA, and Nylon can be used as lung phantoms, while Water Washable Resin has the potential for bone phantoms. Materials (TPU) and Polyethene Terephthalate Glycol (PETG) with variations in thickness and porosity were also tested for the potential of phantom materials, where Samples made from TPU and PETG are suitable for lung, muscle, soft tissue, and spongy bone (Yunianto et al., 2024). Yunianto 2025 has conducted research on EPC materials as kidney organ phantoms. The parameters studied

include material density, CT number, electron density, effective atomic number, and radiation dose, as well as determining the visibility of kidney cancer nodules on variations in CT-Scan exposure voltage, which shows that EPC is suitable as a kidney phantom material (Rachmanto & Akande, 2024; Laksono et al., 2025; Yunianto et al., 2025).

Based on previous research studies related to the use of 3D printer materials as phantom materials for breasts and breast cancer nodules, not much has been done, even though finding materials that have characteristics similar to breast tissue will make it easier for radiologists to analyse and predict the presence of breast cancer. In studying phantom materials, several parameters are used: CT number, dose, material density, relative electron density, effective electron density, electron density per volume, and effective atomic number. The results of these parameters are then compared with references to see the suitability of the characteristics of HIPS breast phantoms with breast organs. The expected goal of this study reflects the fact that so far, in conducting exposure using CT scans on patients who are indicated to have breast cancer, determining the voltage value is still not optimal or only given at the same voltage value, so if it is not right in giving the voltage value, it can happen that the patient should have breast cancer nodules because the exposure is given using a small voltage so that it is not visible in the CT Scan image, with this study it is expected that the magnitude of the voltage value given to the phantom with a certain predicted nodule size can be exposed to the breast phantom first before being exposed to the patient,

The difference with previous studies is that the parameter used to compare with breast organs is only one parameter, namely the CT number value Kunert et al., 2023), while this study uses seven parameters, which can be done with several variations so that the optimal voltage value is obtained. Only then is the voltage value given to the patient. The material used in this study is HIPS, with an infill density of 100%. HIPS is a specific polystyrene because of its opacity and impact resistance, containing 15% to 25% polybutadiene. HIPS is a plastic material that is cheap, easy to produce, and easy to shape. HIPS is widely used because it has glossy, satin or matte results. Apart from that, HIPS is also easily pigmented or coloured (Bhilat et al., 2022).

RESEARCH METHOD

The research was conducted using an experimental method; the research began with a review of similar research, namely reviewing 3D printer materials used as phantom materials for breast organs and lung cancer nodules. The research materials used were: HIPS filament as breast phantom material and PLA filament as cancer nodule material. The tools used were a 3D printer to print the phantom, a CT Scan to reveal the phantom, radiant software to determine the CT number value and INDOSECT software to determine the dose that hit the phantom. In conducting a comparative analysis with breast organ parameters, the parameters used were CT number value, Material density, Electron Density Values ($\boldsymbol{N_e}$), Effective electron density ($\boldsymbol{\rho_{e(EDG)}}$), electron density per volume ($\boldsymbol{\rho_{e(EDV)}}$) Effective atomic number ($\boldsymbol{Z_{eff}}$) And Effective Dose. The parameters resulting from this test are compared with reference data based on ICRU Report 46 (ICRU, 1992), references from Phantom Gammex 467 and previous studies. Overall, the research steps and stages in the analysis can be described as follows.

Breast phantom sample fabrication

Phantom samples were printed with a 3D printer using the FDM technique. The material used to print the samples was HIPS. In the first step, the breast phantom design in (.stl) format was opened using FlashPrint software. The phantom design was cut into five parts to facilitate the cancer nodules' printing process and placement.

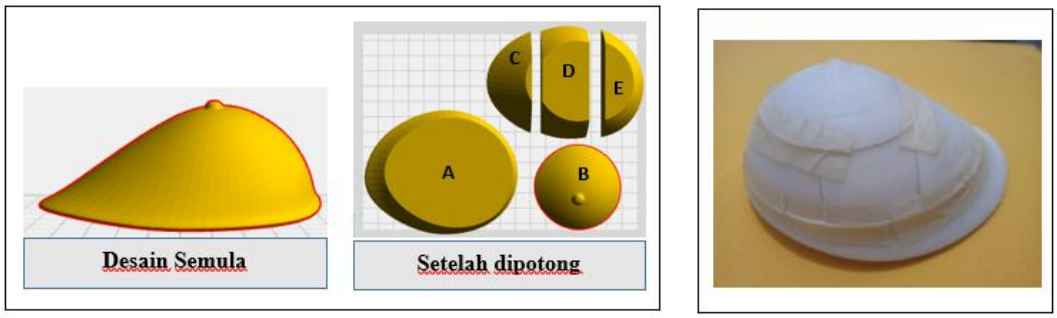

(a) (b)

Figure 1. Breast Phantom (a) Sample Design (b) HIPS Material Sample

The printing of phantom parts A, B, C, D, and E in Figure 1 was done individually. The printing parameters were set using FlashPrint software and saved in (.gcode) format. The infill density was 100% for parts A, B, C, and E, and the infill density was 5% for part D. The samples were printed at a temperature of 230 °C. ℃. The files (.gcode) obtained were then saved on a memory card and entered into the 3D printer. The 3D printer is turned on, and the HIPS filament is installed. The loading process is carried out, and the phantom sample is printed. After five parts of the sample are printed, the cancer nodule made of PLA material is placed in the cavity in sample part D. There are five sizes of cancer nodules, namely 2 mm, 4 mm, 6 mm, 8 mm, and 10 mm. Then, samples of parts A, B, C, D, and E are put together.

Breast Phantom Sample Density Value

Phantom samples were measured using Equation 1. The mass of the sample was weighed using a digital scale. The volume of the sample was calculated by inserting the sample into a beaker filled with distilled water and measuring the increase in volume. The mass and volume measurements of the samples were each repeated five times.

$$\rho = \frac{m}{V} \qquad \text{... (1)}$$

Where ρ is the density of the material (g/ cm^3), m is the mass of the material (g), and V is the volume of the material (cm^3).

Image Acquisition Using CT-Scan Machine

A scan aircraft radiology test was conducted to obtain a digital image of the breast phantom sample, which was used to calculate the CT number, as shown in Figure 2. Before the radiology test was conducted, the CT-scan aircraft specifications were recorded. The sample was placed on the patient's table perpendicularly and parallel to the laser beam on the gantry. The breast phantom sample was given a PLA cancer nodule phantom inside, with variations in phantom size. Nodules are 2 mm, 4 mm, 6 mm, 8 mm, 10 mm. Irradiation was carried out three times with voltage variations of 80 kV, 100 kV, and 120 kV.

Figure 2. Sample irradiation with CT-Scan

Determining CT Number Value

Digital image processing through the RadiAnt DICOM Viewer software obtains the CT number value with the ROI technique. The DICOM file of the CT-Scan sample image is opened using the RadiAnt DICOM Viewer software. The ellipse tool is selected to create an elliptical ROI. ROI is performed at 9 points for the breast phantom image and 5 points for the breast cancer nodule image, with a small uncertainty value and the same ellipse size.

Determining Relative Electron Density Values (N_e), Effective electron density ($\rho_{e(EDG)}$) , electron density per volume ($\rho_{e(EDV)}$) Effective atomic number (Z_{eff}) And Effective Dose.

Electron density measures the probability of electrons in a particular region (Gounhalli et al., 2022). Mathematically, the electron density is as follows·

$$N_e = 1{,}000 + 0{,}001\ N_{CT} \quad if\ N_{CT} < 100 \quad \ldots (2)$$
$$N_e = 1.052 + 0.00048\ N_{CT} \quad , if\ N_{CT} > 100 \quad \ldots (3)$$

Where N_e is the relative electron density value, and N_{CT} is the CT number value (Guswantoro et al., 2020). Effective electron density ($\rho_{e(EDG)}$) It is the number of electrons per unit mass or gram. This electron density is calculated according to the elemental composition of the material. HIPS material has a chemical formula of $(CH_2CH(C_6H_5))$. $\rho_{e(EDG)}$The following equation can calculate EDG (electrons/gram).

$$\rho_{e(EDG)} = N_A \sum_i \frac{W_i\ Z_i}{A_i} \quad \ldots (4)$$

Where N_A is Avogadro's number, $W_i$is the fraction weight, Z_i is the atomic number, and A_i is the atomic mass. The fraction weight can be calculated using Equation 5 (Gounhalli et al., 2022).

$$W_i = \frac{n_i\ A_i}{\sum_i n_i\ A_i} \quad \ldots (5)$$

The magnitude of electron density per volume *($\rho_{e(EDV)}$)* It is based on the density of the material. The magnitude $\rho_{e(EDV)}$or EDV is directly proportional to the density of the material. EDV (electrons/ cm^3) It can be calculated using Equation 6 (Martinez et al., 2012).

$$\rho_{e(EDV)} = \rho \times \rho_{e(EDG)} \quad \ldots (6)$$

Where $\rho_{e(EDV)}$is the electron density per volume, $\rho_{e(EDG)}$is the effective electron density and ρ is the density of the material.

The effective atomic number describes the interaction of photons with the sample material. Z_{eff}. The sample depends on the weight fraction, atomic number, and atomic mass of the elements that make up the sample material. The equation for the effective atomic number is shown in Equation 7.

$$Z_{eff} = \frac{\sum_i \frac{W_i\ Z_i}{A_i}}{\sum_i \frac{W_i}{A_i}} \quad \ldots (7)$$

Where $Z_{eff}$is the effective atomic number, W_i is the weight fraction, A_i is the atomic mass, and Z_i is the atomic number. The radiation dose is determined using a CT-Scan image and dose report from the RadiAnt DICOM Viewer software. Some parameters used from the dose report are tube voltage value (kV), tube current (mA), rotation time (s), pitch factor, and scan length.

RESULTS AND DISCUSSION

Breast Phantom Sample Density Value

The density value of the HIPS phantom material obtained in this study was (0.921 $\pm$ 0.002) g/ cm^3. The density of the breast organ based on ICRU Report 46 data (ICRU, 1992) is 0.950 g/. The

difference in density of the breast cm^3 phantom material with ICRU data is relatively small, namely 3.1%. Then, according to another reference, Miska et al. (2019) made a breast phantom by assuming that the density of the breast is the same as the density of adipose tissue or fat, namely 0.920 g/ cm^3. The difference in density of the breast phantom material with ICRU data is also relatively small, namely 0.1%. Thus, the HIPS breast phantom is appropriate or suitable based on the density value of the material.

CT number Breast Phantom Sample

Breast phantom samples with phantom PLA material nodules were tested using a CT-scan machine. The CT-Scan examination mode used was Head. It was carried out 3 times as exposure with exposure voltage variations of 80 kV, 100 kV, and 120 kV, respectively, current variations of 687 mA, 393 mA, and 265 mA, and rotation time set to 1.0 s. The CT-scan examination results are in the form of images in DICOM files. The DICOM image results are opened using RadiAnt DICOM Viewer software to see the visibility of the nodule and CT number phantom, as in Figures 3,4 and 5. Based on the image results at all exposure voltage variations, a 4 mm nodule was seen on the 152nd slice, 6 mm on the 71st slice, 8 mm on the 111th slice, and 10 mm on the 90th slice. A 2 mm nodule was not seen at any exposure voltage. Then, the CT value of the sample number was searched using the ROI technique, which was carried out on the same slice, namely the 111th slice, at each voltage. ROI was carried out at 9 points and made uniform in size at each kV variation, which was 0.007246 cm^2.

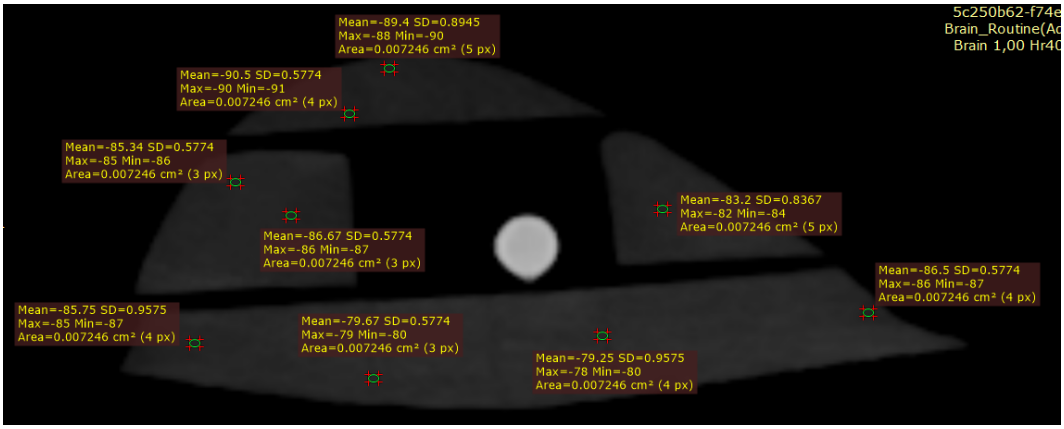

Figure 3. ROI points of CT-Scan images of breast phantom samples at an exposure voltage of 80 kV.

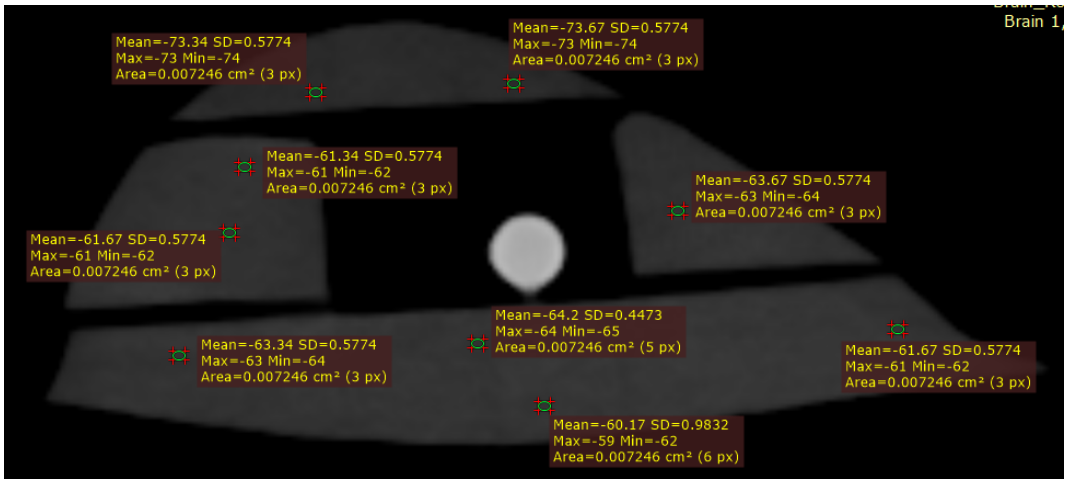

Figure 4. ROI points of CT-Scan images of breast phantom samples at 100 kV exposure voltage.

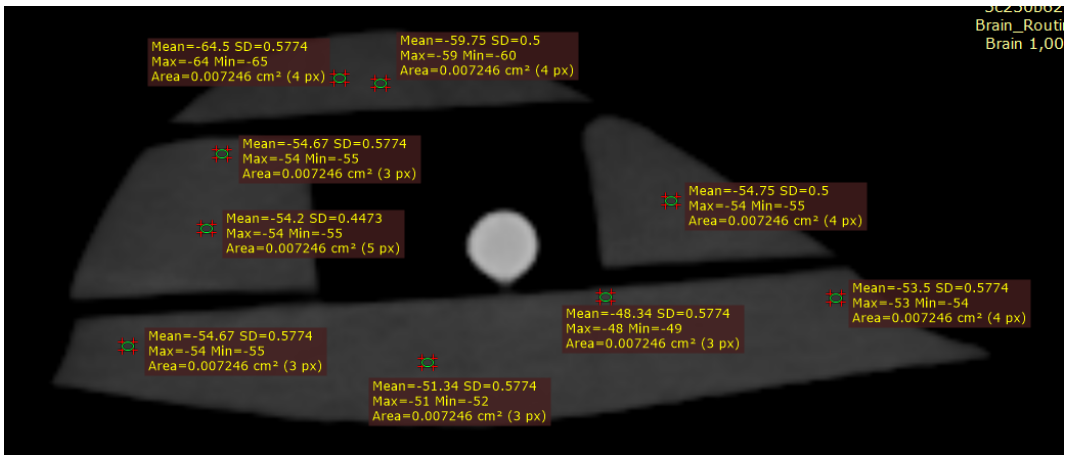

Figure 5. ROI points of CT-Scan images of breast phantom samples at an exposure voltage of 120 kV.

Table 1. CT-Number data of breast phantom samples

Exposure Voltage (kV)	CT Number (HU)	Uncertainty (HU)
80	-85.14	0.25
100	-64.79	0.21
120	-55.08	0.18

Based on Table 1, it can be seen that at exposure voltages of 80 kV, 100 kV, and 120 kV, the CT number values are breast phantom, respectively, namely (-85.14 $\pm$ 0.25) HU, (-64.79 $\pm$ 0.21) HU, and (-55.08 $\pm$ 0.18) HU. Meanwhile, according to the reference, the CT number value of the breast organ is -35 HU to -94 HU (Widyanengsih et al., 2023). This shows that the CT number value of the HIPS breast phantom is according to the CT number value of the reference breast organ.

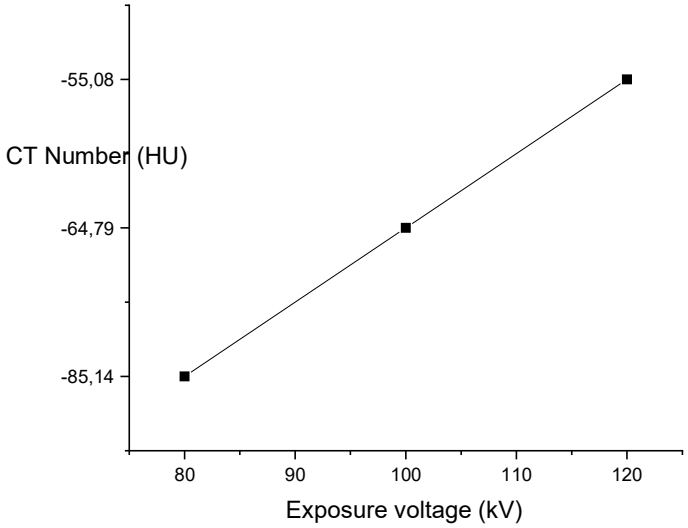

Figure 6. Relationship between exposure voltage and CT number

In Figure 6, you can see that the relationship between changes in the CT number of the breast phantom and changes in exposure voltage is directly proportional. The greater the exposure voltage, the greater the CT number value. This is based on the results of research by Irsal et al. (2021), who concluded that the CT number (HU) value increases with increasing exposure voltage (kV). In addition, ROI was also performed on the PLA breast cancer nodule image. Elliptical ROI was performed at 5 points in 1 slice. ROI was made uniform in size at each kV variation, which was 0.003747 cm^2All nodule sizes. The ROI was performed on the 152nd slice for the 4 mm nodule, the 71st slice for the 6 mm nodule, the 111th slice for the 8 mm nodule, and the 90th slice for the 10 mm nodule.

Based on Table 2, it can be seen that the CT number values of nodules measuring 4 mm, 6 mm, 8 mm, and 10 mm at an exposure voltage of 80 kV are respectively (137.20 ± 2.56) HU, (132.90 ± 1.35) HU, (130.50 ± 0.97) HU, and (131.10 ± 0.91) HU. The CT number values of nodules measuring 4 mm, 6 mm, 8 mm, and 10 mm at an exposure voltage of 100 kV are respectively (141.40 ± 2.05) HU, (133.10 ± 1.16) HU, (131.80 ± 0.77) HU, and (128.87 ± 0.76) HU. The CT number values of nodules measuring 4 mm, 6 mm, 8 mm, and 10 mm at an exposure voltage of 120 kV were respectively (144.90 ± 1.21) HU, (134.77 ± 1.02) HU, (132.90 ± 0.65) HU, and (130.90 ± 0.55) HU. Meanwhile, the CT number values of breast cancer nodules, according to the reference, are 104.54 HU to 167.08 HU. This shows that the CT number values of PLA breast cancer nodule phantoms are based on the CT number values of the reference breast cancer nodules.

Table 2. CT-Number data of cancer nodule phantom samples of the breast

Exposure Voltage (kV)	Nodule Size (mm)	Cancer Nodule Visibility	CT Number (HU)	Uncertainty
80	2	Not visible	-	-
	4	Seen	137.20	2.56
	6	Seen	132.90	1.35
	8	Seen	130.50	0.97
	10	Seen	128.90	0.91
100	2	Not visible	-	-
	4	Seen	141.40	2.05
	6	Seen	133.10	1.16
	8	Seen	131.80	0.77
	10	Seen	129.87	0.76
120	2	Not visible	-	-
	4	Seen	144.90	1.21
	6	Seen	134.77	1.02
	8	Seen	132.90	0.65
	10	Seen	130.90	0.55

Electron density of breast phantom sample

Table 3. Electron density of HIPS breast phantom samples.

Exposure Voltage (kV)	Relative Electron Density	Uncertainty
80	0.915	0.0003
100	0.935	0.0002
120	0.945	0.0002

Table 3 shows that at exposure voltages of 80 kV, 100 kV, and 120 kV, the relative electron density values of the breast phantom are 0.915, 0.935, and 0.945, respectively. Meanwhile, according to the reference, the relative electron density value of the breast organ is 0.96 (Gammex 467 Phantom). This shows that the relative electron density values of the HIPS breast phantom at voltages of 80 kV, 100 kV, and 120 kV have differences with the reference of 4.7%, 2.6%, and 1.6%, respectively. The difference in the relative electron density values of the HIPS breast phantom and the Gammex 467 phantom is relatively small. Hence, the HIPS breast phantom is suitable or appropriate based on its relative electron density value.

Effective electron density (EDG) of breast phantom samples

The result of the EDG value calculation is 3.24 x10^{23} e^{-}/gr. Meanwhile, the EDG value of breast organs based on ICRU data from 1989 and 1992 was 3.33 x10^{23} e^{-}/gr. The difference in EDG values of HIPS breast phantoms with ICRU 1989 and 1992 data is 0.09 x10^{23} e^{-}/gr or 2.7%. Olaosun (2022) in his research stated that the EDG value of the breast organ is 3.29 x10^{23} e^{-}/gr. The difference

between the sample EDG value and that of Olaosun (2022) is 0.05 x10^{23} e^{-}/gror 1.5%. This difference value is relatively small, so based on the EDG value, the HIPS phantom is suitable or appropriate.

Electron density per volume of breast phantom sample

The EDV value of the calculated sample is (3.00 $\pm$ 0.01) x10^{23} e^{-}/cm^{3}. Then, the EDV value of the breast organ based on ICRU report 44 data is 3.18 x 10^{23} e^{-}/cm^{3}. The difference between the EDV value of the sample and the reference is cubed or x10^{23} e^{-}/cm^{3}or 5.7%. Meanwhile, the EDV value of breast adipose tissue based on CIRS 062 is 3.17 x 10^{23} e^{-}/cm^{3}. The difference in EDV values of CIRS 062 breast adipose tissue with the sample is cubed.10^{23} e^{-}/cm^{3}or 5.4%. The EDV value of the breast phantom sample is close to the EDV value of the breast organ from the reference, so based on the EDV value, the HIPS phantom is suitable or appropriate.

Effective atomic number (Z_{eff})

Calculated Z_{eff} value is 3.50, while the value Z_{eff} on ICRU data is 3.28. The difference between the Z_{eff}sample value, and the reference is 0.22 or 6.7%. The Z_{eff} sample value is quite close to the Z_{eff} reference value. This shows that the HIPS breast phantom matches the adipose tissue of the breast organ. So that the HIPS breast phantom sample is suitable or matches based on the effective atomic number value, or Z_{eff}.

Radiation Dose

Radiation dose determination uses CT-scan images and RadiAnt DICOM Viewer software dose reports. Some parameters used from the dose report are tube voltage (kV), tube current (mA), rotation time (s), pitch factor, and scan length, as shown in Table 4.

Table 4. Parameters Used to Calculate $CTDI_{vol}$ and DLP

Tube Voltage (kV)	Tube Current (mA)	Rotation Time (s)	Pitch Factor	Scan Length (cm)
80	378	1.00	0.55	36.095
100	216	1.00	0.55	36.095
120	146	1.00	0.55	36.095

Then, the CT-Scan image and several parameters in Table 4 are used to calculate $CTDI_{vol}$ and DLP using IndoseCT v20b software. Then, the results of the IndoseCT software are compared with the values in the RadiAnt DICOM Viewer software. The results of the values $CTDI_{vol}$ and DLP from the IndoseCT and RadiAnt DICOM Viewer software are shown in Table 5.

Table 5. Results $CTDI_{vol}$ and DLP on IndoseCT and Radiant software

Tube Voltage (kV)	$CTDI_{vol}$IndoseCT (mGy)	$CTDI_{vol}$Radiant (mGy)	DLP IndoseCT (mGy. cm)	DLP Radiant (mGy. cm)
80	40.68	42.70	1468.28	1522.00
100	45.50	46.40	1642.33	1653.00
120	51.48	49.80	1858.20	1775.00

Based on Table 5, it can be seen that the subscript of the IndoseCT software at voltages of 80 kV, 100 kV, and 120 kV are, respectively, 40.68 mGy, 45.50 mGy, and 51.48 mGy. Meanwhile, the values $CTDI_{vol}$ The RadiAnt software at 80 kV, 100 kV, and 120 kV, respectively, produces 42.70 mGy, 46.40 mGy, and 49.80 mGy. Then, the DLP values of the IndoseCT software at voltages of 80 kV, 100 kV, and 120 kV are respectively 1468.28 mGy. cm, 1642.33 mGy. cm, and 1858.20 mGy. cm. Meanwhile, the DLP values of the software RadiAnt at 80 kV, 100 kV, and 120 kV voltages were 1522.00 mGy. cm, 1653.00 mGy. cm, and 1775.00 mGy. cm, respectively. The difference in values $CTDI_{vol}$ and DLP from IndoseCT and RadiAnt is due to the limitations of the collimation input parameters in the IndoseCT software. In the RadiAnt software dose report, the collimation value is 0.6 mm, but in the IndoseCT software, the collimation section does not have a collimation value option of

0.6 mm. So, the input collimation parameters in the IndoseCT software were chosen as the closest, namely 2 mm. This certainly greatly affects the results obtained.

Then, from the IndoseCT software, the effective diameter value (D_{eff}) Moreover, effective doses are also searched. D_{eff} searched in the 111th slice for all variations of tube voltage using the IndoseCT software in the diameter section with the auto method. The value obtained $D_{eff}$for tube voltages of 80 kV, 100 kV, 120 kV is 5.63 cm. D_{eff} only takes into account the geometric size of the object in the image, so that the size of the tube voltage does not affect the value D_{eff}.

The values $CTDI_{vol}$ and D_{eff} are used to find the SSDE value and effective dose in the IndoseCT software. SSDE describes the absorbed dose of the patient/object being irradiated. The effective dose is a dose that is commonly used to estimate the risk of cancer from CT-scan examinations in the future. The results of SSDE and effective dose are shown in Table 6.

Table 6. SSDE values and effective doses

Tube Voltage (kV)	SSDE (mGy)	Effective Dose (mSv)
80	61.33	2.53
100	68.61	2.83
120	77.60	3.20

Table 6 shows that the SSDE values at 80 kV, 100 kV, and 120 kV are 61.33 mGy, 68.61 mGy, and 77.60 mGy, respectively. While the effective dose values at voltages of 80 kV, 100 kV, and 120 kV are 2.53 mSv, 2.83 mSv, and 3.20 mSv, respectively. Based on AAPM Report No. 096 of 2008, the effective dose in chest CT-Scan is 5-7 mSv. This shows that the effective dose value of the breast phantom sample is still within the range. From the data in Table 6, a graph of the relationship between SSDE and effective dose with changes in tube voltage can be made, as shown in Figure 7.

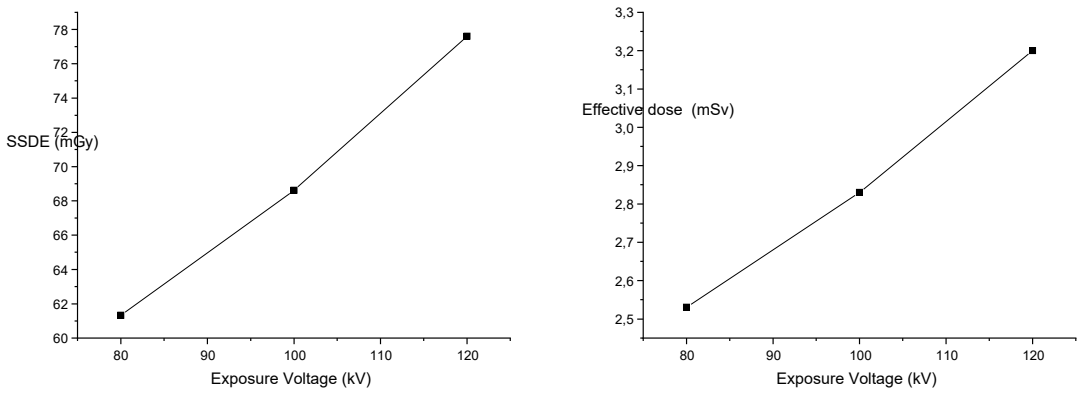

Figure 7. Relationship between exposure voltage and SSDE and effective dose.

From Figure 7, it can be seen that the relationship between SSDE and effective dose with tube voltage is directly proportional. The greater the tube voltage value, the higher the SSDE and effective dose values (Fiarka et al., 2023).

Table 7 shows that the previous research had different materials and several parameters from the research conducted; this research has more parameters, namely seven parameters used, compared to the previous research. In the research that has been conducted, 7 parameters of the test results of HIPS materials have been obtained which have the potential as breast phantoms, from the 7 parameters have been compared with the parameters obtained from the reference, the results obtained for each parameter have almost the same value as the reference, with the error value has been submitted, so it can be concluded that HIPS material can be used as a phantom material for breast organs, when compared with previous studies that to compare phantom materials with organs only use 2 parameters, namely the CT number value and also the density value so that the results of this study have advantages and are better than previous studies, so that the implications of the results of this study have the potential to be implemented as a radiology tool in conducting early detection of breast cancer by first making a mock-

up of the patient's breast organ with a phantom material from HIPS and given breast cancer nodules of various sizes to be exposed.

Table 7. Comparison of the results of phantom development research for the breast organ

Research	Filament/methods	Parameter
Yang et al. (2014)	ABS	CT-Number Value
He et al. (2019)	PVC	Computed Tomography (CT) Attenuation
di Franco et al. (2019)	PVA, ABS and Nylon	Doses Image Quality Assessment
Schopphoven et al. (2019)	Polypropylene	The Anatomical Structures Associated Attenuation
Malliori et al (2020)	Thermoplastic and photopolymer resins	Characteristics Attenuation Refractive Characteristics
Ali et al. (2020)	Multiple resins, VeroClear, TangoPlus and Tissue Matrix	Dose To Glandular Tissue
Lee et al. (2020)	PLA	Doses
Delombaerde et al. (2020)	PLA	Doses Measurement Γ-Analysis
Lee et al. (2021)	Monte Carlo simulation	Bemulating Glandular Adipose Tissues
Mettivier et al. (2022)	ABS, PLA white, PLA orange, PET and NYLON	Monoenergetic X-Ray Linear Attenuation Coefficient
Kunert et al. (2023)	ABS and PMMA	CT-Number Value
Adnan et al. (2023)	HIPS	CT-Number Value
Marashdeh et al. (2023)	Epoxy–Carbopol composites	Attenuation CT properties
Bellara et al. (2024)	PLA, ABS and HIPS	Effective X-Ray Attenuation Coefficient
Grigorova et al. (2024)	soft and flexible silicone rubber	Ultrasound-Based Biopsy
Almalky et al (2024)	Gelatin	Material Density Mechanical Properties
This research	HIPS	CT Number Value Material Density Electron Density Values Effective Electron Density Electron Density Per Volume Effective Atomic Number Effective Dose

The innovation that can be conveyed from this study is the number of parameters used, namely seven parameters and the use of breast cancer nodules, where, to the researcher's knowledge, there has been no research for breast cancer using breast cancer nodule phantoms to detect early breast cancer. The limitation of the study conducted is the variation of the voltage used. Where the study could only do three variations due to the limitations of the CT-Scan tool that we used; if it can be varied more than three voltages, it will be analysed in more detail related to the radiation dose that hits the phantom material and to find out the optimal size of cancer nodules that CT-Scan can detect. Recommendations for further research are to conduct tests for other 3D printer materials with better parameters than the parameters produced from HIPS materials, and to use CT-Scans with more voltage variations.

CONCLUSION

Based on the parameters of material density, CT number, relative electron density, effective electron density (EDG), electron density per volume (EDV), effective atomic number (Z_{eff})When comparing radiation dose with the reference, it can be concluded that the characteristics of the HIPS breast phantom are similar to those of the breast organ so that the HIPS material can be used as a breast phantom material. Nodules with diameters of 4 mm, 6 mm, 8 mm, and 10 mm are visible on CT-scan images with exposure voltage parameters of 80 kV, 100 kV, and 120 kV. While nodules with a diameter of 2 mm are not visible on CT-Scan images with exposure voltage parameters of 80 kV, 100 kV, and 120 kV, in the implementation of breast cancer exposure, nodules measuring less than 2 mm are not visible and it is recommended to use an exposure voltage of more than 120 kV to estimate the size of small nodules. The research that has been conducted previously only focused on the CT number value and dose value parameters. In contrast, this research uses seven parameters, which are expected to enable subsequent research to conduct studies on other materials or other organs using the parameters used in this research.

ACKNOWLEDGMENTS

The author would like to thank LPPM UNS for providing funding through the 2024 Research Group Grant with contract Number 194.2/UN27.22/PT.01.03/2024 and UNS Hospital for cooperation and permission to use facilities for research.

AUTHOR CONTRIBUTIONS

Conceptualization, Yunianto, M. and Anwar, F.; Methodology, Yunianto M; Validation, Devi, N A, and Cindyana, A; Formal Analysis, Anwar, F.; Investigation, Yunianto, M.; Resources, Cidyana, A.; Data Curation, Yunianto, M.; Writing – Original Draft Preparation, Anwar, F.; Writing – Review & Editing, Yunianto, M.; Visualization, Devi, N A, and Cindyana, A.; Supervision, Yunianto, M.; Project Administration, Cindyana, A.; Funding Acquisition, Anwar, F.

CONFLICTS OF INTEREST

The author(s) declare no conflict of interest.

USE OF ARTIFICIAL INTELLIGENCE (AI)-ASSISTED TECHNOLOGY

The authors declare that no artificial intelligence (AI) tools were used in the generation, analysis, or writing of this manuscript. All aspects of the research, including data collection, interpretation, and manuscript preparation, were carried out entirely by the authors without the assistance of AI-based technologies.

REFERENCES

Ali, A., Wahab, R., Huynh, J., Wake, N., & Mahoney, M. (2020). Imaging properties of 3D printed breast phantoms for lesion localization and Core needle biopsy training. *3D Printing in Medicine, 6*, 1-6. https://doi.org/10.1186/s41205-020-00058-5

Almalki, H., Marashdeh, M. W., Alsuhybani, M., & Almurayshid, M. (2024). Evaluation of radiation attenuation properties of breast equivalent phantom material made of gelatin material in mammographic X-ray energies. *Journal of Radiation Research and Applied Sciences*, *17*(1), 100817. https://doi.org/10.1016/j.jrras.2024.100817

Anwar, Y., Zarzani, TR, & Chermanto. (2023). Legal responsibility of medical physicists for quality of radiology operational permits at bhayangkara hospital, *Banda Aceh. Sibatik Journal* , *2*(8), 2263-2282 . https://doi.org/10.54443/sibatik.v2i8.1196

Belarra, A., Chevalier, M., Garayoa, J., Hernández-Girón, I., & Valverde, J. (2024, May). Measuring effective attenuation coefficients of 3D printing materials for anthropomorphic breast phantoms. *In 17th International Workshop on Breast Imaging* (IWBI 2024) (Vol. 13174, pp. 352-360). SPIE. https://doi.org/10.1117/12.3027031

Byng, J. W., Mainprize, J. G., & Yaffe, M. J. (1998). X-ray characterization of breast phantom materials. *Physics in Medicine & Biology*, *43*(5), 1367. https://doi.org/10.1088/0031-9155/43/5/026

Carton, A. K., Bakic, P., Ullberg, C., Derand, H., & Maidment, A. D. (2011). Development of a physical 3D anthropomorphic breast phantom. *Medical physics*, *38*(2), 891-896.

https://doi.org/10.1118/1.3533896

Cuong, NLQ, Minh, NH, Cuong, HM, Quoc, PN, Van Anh, NH, & Van Hieu, N. (2018). Porosity estimation from High-Resolution CT Scan images of rock samples using hounsfield units. *Open Journal of Geology*, *8*(10), 101- 109. https://doi.org/10.4236/ojg.2018.810061

Delombaerde, L., Petillion, S., Weltens, C., De Roover, R., Reynders, T., & Depuydt, T. (2020). Development of 3D-printed breast phantoms for end-to-end testing of whole breast volumetric arc radiotherapy. *Journal of Applied Clinical Medical Physics*, *21*(8), 315-320. https://doi.org/10.1002/acm2.12976

di Franco, F., Mettivier, G., Sarno, A., Varallo, A., & Russo, P. (2019). Manufacturing of physical breast phantoms with 3D printing technology for X-ray breast imaging. In 2019 IEEE Nuclear Science Symposium and Medical Imaging Conference (NSS/MIC) (pp. 1-5). IEEE https://doi.org/10.1109/NSS/MIC42101.2019.9059986

Di Meo, S., Cannatà, A., Morganti, S., Matrone, G., & Pasian, M. (2022). On the dielectric and mechanical characterization of tissue-mimicking breast phantoms. *Physics in Medicine & Biology*, *67*(15), 155018. https://doi.org/10.1088/1361-6560/ac7bcc

Dukov, N., Bliznakova, K., Teneva, T., Marinov, S., Bakic, P., Bosmans, H., & Bliznakov, Z. (2021). Experimental evaluation of physical breast phantoms for 2D and 3D breast x-ray imaging techniques. In 8th European Medical and Biological Engineering Conference: Proceedings of the EMBEC 2020, November 29–December 3, 2020 Portorož, Slovenia (pp. 544-552). Springer International Publishing. https://doi.org/10.1007/978-3-030-64610-3_62

Endra, K., & Villaflor, G. M. (2024). Integration of the POE model and metaphoral thinking in student worksheets: Improving mathematical reasoning abilities in the modern education era. *Journal of Educational Technology and Learning Creativity*, *2*(1), 41-53. https://doi.org/10.37251/jetlc.v2i1.981.

Esposito, G., Mettivier, G., Bliznakova, K., Bliznakov, Z., Bosmans, H., Bravin, A., & Russo, P. (2019). Investigation of the refractive index decrement of 3D printing materials for manufacturing breast phantoms for phase contrast imaging. *Physics in Medicine & Biology, 64*(7), 075008. https://doi.org/10.1088/1361-6560/ab0670

Fiarka, F., Oktamuliani, S., & Nuraeni, N. (2023). Effect of voltage on CTDIvol Value, dose length product and effective dose in computed tomography (CT) abdomen examination: Study at Dr. M. Djamil central general hospital. *Journal of Physics Unand, 12*(4), 591-597. https://doi.org/10.25077/jfu.12.4.591-597.2023

Globocan. (2022). Cancer Incident in Indonesia. International Agency for Research on Cancer, 858: 1–2.

Gómez, Á. ML, & Mourão, A.P. (2022). Study of materials for the construction of phantoms for radiodiagnostic tests. In Proceedings of the 5. *SENCIR: Brazilian National Week on Nuclear and Energy Engineering and Radiation Sciences*, 1–9. https://doi.org/10.37885/221110974

Gounhalli, S. G., Basavaraj, S., & Hanagodimath, S. M. (2022). Mass attenuation coefficients, effective atomic number, electron density, and kerma of BBPD and BBPO Organic Molecules. *Journal of the Maharaja Sayajirao University of Baroda* , *56*(2), 9-18.

Gusriani, Umami, N., Noviyanti, NI, Rusmiati, & Fitri, G. (2023). Early detection of breast cancer with clinical breast examination (SADARI). *Borneo Community Service Journal*, *7*(1), 51-55. https://doi.org/10.35334/jpmb.v7i1.3326

Grigorova, N., Kaloyanova, D., Dukov, N., & Bliznakova, K. (2024, November). Ultrasound breast phantom for breast biopsy training. *In 2024 E-Health and Bioengineering Conference* (EHB) (1-4). IEEE. https://doi.org/10.1109/EHB64556.2024.10805633

Guswantoro, T., Supratman, AS, & Asih, IS (2020). Characterization of alginate as a soft tissue equivalent material for radiotherapy. *EduMatSains*: *Journal of Education, Mathematics and Science*, 4(2), 125-138. https://doi.org/10.33541/edumatsains.v4i2.1378

Habibi, M. W., Jiyane, L., & Özşen, Z. (2024). Learning revolution: The positive impact of computer simulations on science achievement in madrasah ibtidaiyah. *Journal of Educational Technology and Learning Creativity*, *2*(1), 13-19. https://doi.org/10.37251/jetlc.v2i1.976.

Hatamikia, S., Kronreif, G., Unger, A., Oberoi, G., Attorney, L., Unger, E., & Lorenz, A. (2022). 3D Printed Patient-Specific thorax phantom with realistic heterogeneous bone radiopacity using filament printer technology. *Zeitschrift für Medizinische Physik*, 1(1), 1-15. https://doi.org/10.1016/j.zemedi.2022.02.001

Halimah, H., Putri , D. E., Wulandari, W., Adewumi, S. E., & Arce-Calderón, X. (2024). Contextual pop up book as an innovative learning media in social science subjects in elementary schools. *Journal of Educational Technology and Learning Creativity*, *2*(2), 209-216. https://doi.org/10.37251/jetlc.v2i2.1121.

Hermanto, A., Aridamayanti, BG, Iswahyudi, UA (2023). The Relationship between Active and Passive Smokers and Knowledge of Lung Cancer in Students at SMAN 1 Wongsorejo. *Profesional Health Journal*, 4(2): 281-286. http://dx.doi.org/10.54832/phj.v4i2.383

He, Y., Liu, Y., Dyer, B. A., Boone, J. M., Liu, S., Chen, T., & Qiu, J. (2019). 3D-printed breast phantom for multi-purpose and multi-modality imaging. Quantitative imaging in medicine and surgery, *9*(1), 63. https://doi.org/10.21037/qims.2019.01.05

Irsal, M., Nurbaiti, Mukhtar, AN, Gunawati, S., & Hidayat, W. (2021). The Effect of Tube Voltage on Image Quality in Head Computed Tomography Examination using Iterative Reconstruction. *Journal of Physics Theory and Applications*, *9*(1):103-110. http://dx.doi.org/10.23960/jtaf.v9i1.2715

Jarnawi, M., Haeruddin, H., Werdhiana, I. K., Syamsuriwal, S., & Mu'aziyah, S. E. S. (2025). Integrating thinking styles into differentiated instruction: enhancing learning outcomes in science education. *Integrated Science Education Journal*, *6*(1), 47-53. https://doi.org/10.37251/isej.v6i1.1328

Katsikari, K., Francis, N., Maalej, N., Pitsalidis, C., & Raja, A. Y. (2024). 3D-Printed anthropomorphic phantom framework for spectral photon-counting CT: A breast phantom application. IEEE Access. https://doi.org/10.1109/ACCESS.2024.3521476

Keenan, K. E., Wilmes, L. J., Aliu, S. O., Newitt, D. C., Jones, E. F., Boss, M. A., ... & Hylton, N. M. (2016). Design of a breast phantom for quantitative MRI. *Journal of Magnetic Resonance Imaging*, *44*(3), 610-619. https://doi.org/10.1002/jmri.25214

Khoirot, RM, Hakim, MH, Alam, Y., & Sekar, R. (2023). Analysis of DRL values of esak/inak parameters of thorax AP/PA X-Ray canon examination. *Journal of Science Nusantara*, *3*(2): 61-68. https://doi.org/10.28926/jsnu.v3i2.1041

Kunert , P. , Schlattl, H. , Trinkl .S , Glussani, A., Klein, L., Janich, M., Reichert, D., & Brix, G. (2023). Reproduction of a conventional anthropomorphic female chest phantom by 3D-Printing: Comparison of image contrasts and absorbed doses in ct. *Med Phys*, *50*, 4734 – 4743. https://doi.org/10.1002/mp.16587

Laksono, P. J., Suhadi, S., & Efriani, A. (2025). Unveiling STEM education conceptions: Insights from pre-service mathematics and science teachers. *Integrated Science Education Journal*, *6*(1), 54-61. https://doi.org/10.37251/isej.v6i1.1387

Lee, J. S., Jo, Y. I., Kang, Y. R., Kye, Y. U., Il, P., & Lee, D. Y. (2020). Filament material evaluation for breast phantom fabrication using three-dimensional printing. *Nuclear Technology and Radiation Protection, 35*(4), 372-379. https://doi.org/10.2298/NTRP2004372L

Lee, D. Y., Jo, Y. I., & Yang, S. H. (2021). Development of breast phantoms using a 3D printer and glandular dose evaluation. *Journal of Applied Clinical Medical Physics*, *22*(10), 270-277. https://doi.org/10.1002/acm2.13408

Leonov, D., Venidiktova, D., Costa-Júnior, J. F. S., Nasibullina, A., Tarasova, O., Pashinceva, K., & Saikia, M. J. (2024). Development of an anatomical breast phantom from polyvinyl chloride plastisol with lesions of various shape, elasticity and echogenicity for teaching ultrasound examination. *International Journal of Computer Assisted Radiology and Surgery*, *19*(1), 151-161. https://doi.org/10.1007/s11548-023-02911-4

Listiyani, I., Nismayanti, A., Maskur, Kasman, Ulum, MS, Rahman, A., & Samad, S. (2021). Noise Level Analysis of CT-Scan Image Results on Head Phantom with Variations in Tube Voltage and Slice Thickness. *Gravitation* , *20*(1), 5–9. http://dx.doi.org/10.22487/gravitasi.v20i1.15517

Mettivier, G., Sarno, A., Varallo, A., & Russo, P. (2022). Attenuation coefficient in the energy range 14–36 keV of 3D printing materials for physical breast phantoms. *Physics in Medicine & Biology*, *67*(17), https://doi.org/175012. 10.1088/1361-6560/ac8966

Malliori, A., Daskalaki, A., Dermitzakis, A., & Pallikarakis, N. (2020). Development of physical breast phantoms for X-ray imaging employing 3D printing techniques. *The Open Medical Imaging Journal*, *12*(1). http://dx.doi.org/10.2174/1874347102012010001

Marashdeh, M., & Abdulkarim, M. (2023). Determination of the attenuation coefficients of epoxy resin with carbopol polymer as a breast phantom material at low photon energy range. *Polymers*,

15(12), 2645. https://doi.org/10.3390/polym15122645

Martinez, L.C., Calzado, A., Rodriguez, C., Gilarranz, R., & Manzanas, M.J.(2012). A parametrization of the CT number of a substance and its use for stoichiometric calibration. *Physica Medica*, *28*(1), 33-42. https://doi.org/10.1016/j.ejmp.2011.02.001

Ock, J., Lee, S., Kim, T., Hong, D., Kim, M., Ko, B. S., & Kim, N. (2021). Accuracy evaluation of a 3D printing surgical guide for breast-conserving surgery using a realistic breast phantom. *Computers in Biology and Medicine*, *137*, 104784. https://doi.org/10.1016/j.compbiomed.2021.104784

Plummer, M., de Martel, C., Vignat, J., Ferlay, J., Bray, F., & Franceschi, S. (2016). Global burden of cancers attributable to infections in 2012: a synthetic analysis. *The Lancet Global Health*, *4*(9), e609-e616. https://doi.org/10.1016/s2214-109x(16)30143-7

Pohan, M. Y., Siregar, T. Z., & Panjaitan, B. (2022). Analisa paparan radiasi pada instalasi radiologi di rumah sakit islam malahayati medan tahun 2021 [Analysis of radiation exposure in the radiology installation at the Malangayati Islamic Hospital, Medan in 2021]. *Jurnal Ilmiah Ilmu Terapan Universitas Jambi, 6*(1), 66–72. https://doi.org/10.22437/jiituj.v6i1.19333

Pratiwi, RF, Pulungan, ES, & Andini, D. (2023). The effect of exposure factors on the quality of radiographic images in thorax examination. *Indonesian Radiographer Journal*, 6(1), 38-41. https://doi.org/10.55451/jri.v6i1.173

Pritchard, P.E. (1992). Studies on the bread-improving mechanism of fungal alpha-amylase. *Journal of Biological Education, 26*(1), 14–17. https://doi.org/10.1037/0012-1649.44.4.1055.

Rachmanto, T. B., & Akande, I. O. (2024). Utilization of information technology in increasing the effectiveness of citizenship learning. *Journal of Educational Technology and Learning Creativity*, *2*(2), 217-222. https://doi.org/10.37251/jetlc.v2i2.1140.

Rifda, DZ, Shaluhiyah, Z., & Surjoputro. (2023). Phenomenological study of breast cancer patients in an effort to improve quality of life: Literature review. *Indonesian Health Promotion Publication Media, 6*(8): 1495-1500. https://doi.org/10.56338/mppki.v6i8.3513

Riza, EI, Budiyantoro, C., & Nugroho, AW (2020). Increasing flexural strength of 3D printing products made of PETG with optimization of process parameters using the taguchi method. *Media Mesin: Jurnal Teknik Mesin , 2*1(2), 66-75. https://doi.org/10.23917/mesin.v21i2.10856

Sindi, R., Wong, Y. H., Yeong, C. H., & Sun, Z. (2020). Development of patient-specific 3D-printed breast phantom using silicone and peanut oils for magnetic resonance imaging. *Quantitative imaging in medicine and surgery*, *10*(6), 1237. https://doi.org/10.21037/qims-20-251

Surahmi, N., Sari, K., Ulliana, U., & Badari, M. (2023). Level of accuracy of intraoral examination in impaction cases using general purpose devices in radiology installation. *Journal of Health Research, 15*(2), 246-252. https://doi.org/10.34011/juriskesbdg.v15i2.2134

Spytska, L. (2025). Digital technology and mental health: Unveiling the psychological impact of modern digital habits. *Jurnal Ilmiah Ilmu Terapan Universitas Jambi*, *9*(1), 348–365. https://doi.org/10.22437/jiituj.v9i1.38238

Schopphoven, S., Cavael, P., Bock, K., Fiebich, M., & Mäder, U. (2019). Breast phantoms for 2D digital mammography with realistic anatomical structures and attenuation characteristics based on clinical images using 3D printing. *Physics in Medicine & Biology, 64*(21), 215005. https://doi.org/10.1088/1361-6560/ab3f6a

Utami, N. W., & Saptiari, N. N. (2020). Penerapan data mining untuk klasifikasi penyebab kematian menggunakan algoritma support vector machine. *Jurnal Ilmiah Ilmu Terapan Universitas Jambi, 4*(2), 234–240. https://doi.org/10.22437/jiituj.v4i2.13268

Widyanengsih, E., Fitria, LN, Jabar, MA, Dzulfiana, N., A, SR, Cahyati, SAW, Salsabila, T., & Yuniarsih, N. (2023). Review article: Nanoparticle drug delivery system in cancer cells. *Journal of Education and Counselling, 5*(1), 1133–1138. https://doi.org/10.31004/jpdk.v5i1.11122

Yang, K., Burkett, G., & Boone, J. M. (2014). A breast-specific, negligible-dose scatter correction technique for dedicated cone-beam breast CT: A Physics-Based approach to improve Hounsfield Unit Accuracy. *Physics In Medicine & Biology*, *59*(21), 487–505. https://doi.org/10.1088/0031-9155/59/21/6487

Yunianto, M., & Ranny, LN (2025). Study of EPC type 3D printer materials as a kidney organ phantom with variations in CT-Scan exposure voltage and kidney cancer nodule size. In Journal of Physics: Conference Series (Vol. 2945, No. 1, p. 012027*). IOP Publishing*. https://doi.org/10.1088/1742-6596/2945/1/012027

Yunianto, M., Cari, C., & Sari, APK (2024). Analysis of the effect of changes in thickness and infill density of thermoplastic polyurethane and polyethylene terephthalate glycol materials as a Radiological Phantom. *Aceh International Journal of Science and Technology*, *13*(2). https://doi.org/10.13170/aijst.13.2.40201

Yunianto, M., Yani, S., Anwar, F., Suparmi, A., Cari, C., Sarwidi, S., & Ardyanto, TD (2024). Comparison of CT number and electron density in 3D printing materials for phantom applications. In *AIP Conference Proceedings* (Vol. 3074, No. 1). AIP Publishing. https://doi.org/10.1063/5.0211295